Journal of chemical & engineering data

Article

pubs.acs.org/jced

Experiments and Correlations of the Vapor−Liquid Equilibria for Carbon Monoxide + Propionic Acid and Carbon Monoxide + Methyl Formate Systems

Li Yanfen,[†] Yuan Pingfang,[†] Ji Jia,[†,‡] Zhou Jianguo,[†,§] Zhu Rongjiao,*[,†] and Tian Yiling[†]

[†]Department of Chemistry, School of Science, Tianjin University, Tianjin, 300072, China

[‡]The Library of Civil Aviation University of China, Tianjin, 300300, China

[§]Department of Materials Science and Engineering, Tianjin Institute of Urban Construction, Tianjin, 300384, China

ABSTRACT: Vapor−liquid equilibrium data p, T, x, ρ, and V_m at (293.2, 313.2, 333.2, and 353.2) K and pressures between (1.39 and 9.96) MPa for the binary systems of carbon monoxide (CO) + propionic acid (PA) and carbon monoxide + methyl formate (MF) were reported. The equilibria were measured using a variable-volume cylindrical autoclave. The experimental data were modeled using the Peng−Robinson (PR) equation of state (EOS) and Peng−Robinson−Stryjek−Vera (PRSV) equation of state with van der Waals I or Panagiotopoulos−Reid mixing rules. The compared results showed a satisfactory agreement between the correlated and the experimental data. The binary interaction parameters were also obtained. At the same time, the Henry's coefficient, molar solution enthalpy, and molar solution entropy of CO in propionic acid and methyl formate were calculated.

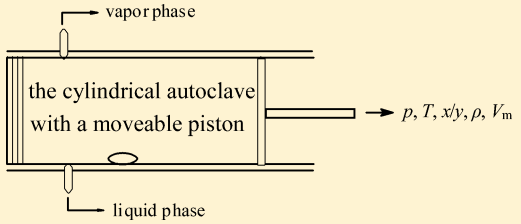

INTRODUCTION

Propionic acid (PA) and its calcium, sodium, and potassium salts are widely used as preservatives in animal feed and human foods, and it is also an important chemical intermediate in the synthesis of cellulose fibers, herbicides, perfumes, and pharmaceuticals.[1] Methyl formate (MF) is a versatile chemical precursor to synthesize chemicals, such as formic acid, acetic acid, acetaldehyde, methyl acetate, ethylene glycol, and formamide.[2] Many methods were applied in the synthesis of PA and MF in industry,[3−8] among which carbonylation of carbon monoxide is one of the most important routes.[9]

Vapor−liquid equilibrium measurement at high-pressure phase equilibrium data play an essential role in thermodynamics, not only for their use in the designment and separation processes but also for their importance in the testing and extension of fluid mixture theories.[10] As the synthesis pressures are usually from (2.00 to 8.00) MPa, the vapor−liquid equilibrium data for the binary systems of carbon monoxide (CO) + propionic acid (PA) and carbon monoxide (CO) + methyl formate (MF) were investigated at temperatures from (293.2 to 353.2) K and pressures from (1.39 to 9.96) MPa.

EXPERIMENTAL SECTION

Materials and Their Purities. CO was provided by Tianjin Special Gas Limited Company (China) with a molar fraction of 0.999. The gas was dried with anhydrous $CaCl_2$ powder. PA and MF were supplied by Aladdin Reagent Company with a mass fraction of 0.998. They were used as received without further purification but degassed for 2 h at low temperatures (0 °C) and pressures (30 kPa).

Experimental Apparatus and Procedures. The experiments were carried out in a cylindrical autoclave with a moveable piston which is shown in Figure 1. It was similar to

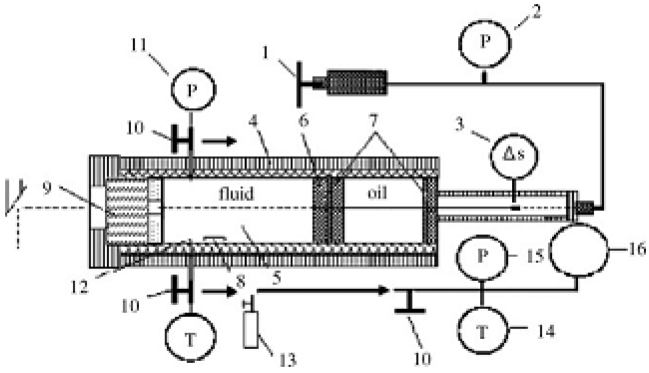

Figure 1. Schematic diagram of the high-pressure apparatus: (1) screw-driven pump, (2) pressure meter, (3) Hall probe, (4) heat jacket, (5) autoclave, (6) piston, (7) O-ring, (8) stirrer, (9) quartz window, (10) sample valves, (11) pressure sensor, (12) thermocouple, (13) small steel vessel, (14) thermometer, (15) vacuum meter, (16) glass bulb.

that in reported in literature.[11−13] The main part of the apparatus is a cylindrical high-pressure cell (length 307 mm, i.d. 20 mm, o.d. 78 mm, made of Ni stainless steel). The piston is between the contents and the pressure medium (oil). There is a Hall probe (model SS541AT) connected to the piston which

Received: November 28, 2011
Accepted: May 23, 2012
Published: June 8, 2012

dx.doi.org/10.1021/je3001969 | J. Chem. Eng. Data 2012, 57, 1887−1893

can measure the position of the piston. The uncertainty of position was ± 0.1 mm. The pressure was realized manually with an operated screw-driven pump and was measured with a pressure sensor (model CYB-20S). The temperature was realized by the circulated water (when T < 353.2 K) or a heating jacket (when T > 353.2 K). The temperature was measured with a calibrated chromel-alumel thermocouple. The uncertainties of temperature and pressure can be controlled within ± 0.1 K and ± 0.01 MPa, respectively.

First, the liquid (PA or MF) and carbon monoxide were charged into the vacuum cell. To minimize the temperature inhomogeneities, the contents were stirred by a magnetic stirrer in the cell. The phase equilibrium was achieved when the pressure and temperature of the system kept invariant for 2 h after stirring. Then the sample of the liquid phase was taken from the lower valve into a small steel vessel which had been evacuated and weighed previously. During this sampling process, the phase equilibrium was still maintained, as the pressure of the system kept constant with the help of the operated screw-driven pump. The total mass of the sample was weighed using an electric balance with an accuracy of 0.0001 g. The process of the vapor phase sampling was similar to that of the liquid phase. The only difference was sampling from the upper valve. Stirring the content, the liquid and vapor phases were sampled again after the phase equilibrium was maintained for 0.5 h. Then the pressure and temperature were changed to another value.

The mole fraction was determined by the desorption method. The sample vessel was cooled in the mixture of ice and water. Then it was connected to an evacuated glass bulb, the volume of which was known. The temperature of the bulb was measured by a thermometer with a precision of 0.1 °C. The pressure inside the bulb was measured with an absolute-pressure meter with a precision of 10 Pa. The more volatile component (CO) would be separated to the glass bulb after opening the valve of the sample vessel. Then the sample left was weighed, and the value of the absolute-pressure meter was recorded. The amount of CO can be calculated by the mass difference method (i.e., the total mass of sample minus the mass left after CO desorbed) and the equation of state method ($n = \Delta PV/RT$). The amount of the heavy component can be determined by the mass difference method (i.e., the mass of vessel left after CO desorbed minus the mass of the vessel before sampling). The volume of the taken sample was determined by measuring the distance between the positions of the piston before and after taking the sample, Δl, and the known inner diameter of the autoclave. The density was obtained by the appropriate mass divided by the volume of the sample taken in each phase.

CORRELATION

The Peng−Robinson (PR) and the Peng−Robinson−Stryjek−Vera (PRSV) equations of state (EOS) coupled with the van der Waals I or the Panagiotopoulos−Reid mixing rules[14,15] were used to correlate the experimental data.

The PR equation of state has the following form:

$$p = \frac{RT}{V_m - b} - \frac{a(T)}{V_m(V_m + b) + b(V_m - b)} \tag{1}$$

with

$$a(T) = a_c\alpha(T) = \frac{0.45724R^2T_c^2\alpha(T)}{p_c} \tag{2}$$

$$b = \frac{0.07780RT_c}{p_c} \tag{3}$$

$$\alpha(T) = [1 + k(1 - T_r^{0.5})]^2 \tag{4}$$

$$T_r = \frac{T}{T_c} \tag{5}$$

$$k = 0.3746 + 1.54226\omega - 0.26992\omega^2 \tag{6}$$

The PRSV equation of state is improved from the PR equation of state. The difference between these two equations is just the expression of k. In PRSV equation of state, k is expressed as the following:

$$k = k_0 + k_1(1 + T_r^{0.5})(0.7 - T_r) \tag{7}$$

$$k_0 = 0.378893 + 1.4897153\omega - 0.17131848\omega^2 + 0.0196554\omega^3 \tag{8}$$

where T_c and p_c are the critical temperature and critical pressure of the pure components, respectively, ω is the acentric factor, and k_1 is a specific pure compound parameter. The critical data T_c, p_c, ω, and k_1 are listed in Table 1, taken from refs 16 and 17.

Table 1. Physical Properties of Pure Substances[16,17]

substance	T_c/K	p_c/MPa	ω	k_1[a]
PA	598.50	4.67	0.536	0.18206
MF	487.20	6.00	0.254	0.41077
CO	132.80	3.49	0.053	−0.02157

[a] k_1 is estimated in this work with the data from ref 17.

For a binary mixture, the van der Waals I mixing rule was used as follows:

$$a_M = \sum_i \sum_j x_i x_j (a_i a_j)^{1/2}(1 - k_{ij}) \tag{9}$$

$$b_M = \sum_i x_i b_i \tag{10}$$

here x_i are mole fractions.

The Panagiotopoulos−Reid mixing rule was used as follows:

$$a_M = \sum_i \sum_j x_i x_j (a_i a_j)^{1/2}[1 - k_{ij} + (k_{ij} - k_{ji})x_i] \tag{11}$$

$$b_M = \sum_i x_i b_i \tag{12}$$

where k_{ij} and k_{ji} are the binary interaction parameters.

The objective function is as follows:

$$F = \sum_{i=1}^{N}\left(\frac{p - p_{cal}}{p}\right)^2 + \sum_{i=1}^{N}\sum_{j=1}^{M}\left(\frac{y_j - y_{j,cal}}{y_j}\right)^2 \tag{13}$$

where the subscript cal represents calculated values. N represents the number of the experimental points, and M represents the number of the components.

RESULTS AND DISCUSSION

Table 2 presents the experimental vapor−liquid equilibrium data p, T, x, ρ, and V_m at (293.2, 313.2, 333.2, and 353.2) K and pressures between (1.39 and 9.96) MPa for the binary systems

dx.doi.org/10.1021/je3001969 | J. Chem. Eng. Data 2012, 57, 1887−1893

Table 2. Experimental Equilibrium Data for the Systems CO (1) + PA (2) and CO (1) + MF (2) at Different T and p Values (Temperatures and Pressures)

CO (1) + PA (2)								
p^a / MPa	$x_1{}^b$	$\rho_l{}^c$ / g·cm^{-3}	$V_{m,l}$ / cm^3·mol^{-1}	$y_1{}^b$	$\rho_g{}^c$ / g·cm^{-3}	$V_{m,g}$ / cm^3·mol^{-1}	K_1	K_2
				T/K = 293.2				
1.75	0.0156	0.9882	74.24	0.9985	0.0231	1215.11	64.03	0.001
2.53	0.0211	0.9831	74.36	0.9981	0.0301	933.14	47.28	0.003
2.98	0.0237	0.9783	74.61	0.9977	0.0366	767.92	42.06	0.003
4.05	0.0298	0.9705	74.92	0.9966	0.0461	610.77	33.41	0.005
4.75	0.0353	0.9623	75.29	0.9959	0.0537	524.93	29.00	0.006
5.72	0.0418	0.9504	75.92	0.9945	0.0651	434.00	24.35	0.007
6.73	0.0487	0.9372	76.65	0.9918	0.0752	377.37	20.37	0.009
7.80	0.0596	0.9197	77.56	0.9871	0.0897	318.78	18.14	0.010
				T/K = 313.2				
1.50	0.0121	0.9854	74.61	0.9971	0.0174	1616.88	82.49	0.002
1.96	0.0146	0.9783	75.04	0.9973	0.0207	1358.67	68.31	0.003
2.90	0.0202	0.9726	75.21	0.9967	0.0311	905.21	49.29	0.004
3.88	0.0269	0.9651	75.47	0.9958	0.0417	676.10	36.93	0.007
4.80	0.0311	0.9574	75.88	0.9946	0.0502	562.73	31.92	0.008
5.85	0.0387	0.9452	76.49	0.9919	0.0627	452.52	26.28	0.009
6.88	0.0465	0.9312	77.25	0.9889	0.0703	405.57	22.25	0.011
7.78	0.0557	0.9133	78.30	0.9846	0.0842	340.97	19.48	0.013
				T/K = 333.2				
1.55	0.0105	0.9774	75.30	0.9960	0.0112	2516.46	94.95	0.003
1.91	0.0125	0.9712	75.68	0.9963	0.0150	1878.03	79.70	0.004
2.88	0.0179	0.9649	75.92	0.9955	0.0259	1089.09	55.53	0.006
3.89	0.0240	0.9580	76.17	0.9939	0.0371	762.29	41.34	0.008
4.85	0.0280	0.9498	76.64	0.9923	0.0466	608.47	35.35	0.010
5.75	0.0341	0.9385	77.26	0.9899	0.0565	503.81	29.00	0.012
6.86	0.0418	0.9253	77.98	0.9861	0.0666	430.04	23.62	0.014
7.87	0.0508	0.9077	79.03	0.9789	0.0806	359.46	20.91	0.016
				T/K = 353.2				
1.39	0.0082	0.9684	76.11	0.9943	0.0062	4558.49	121.46	0.004
1.96	0.0108	0.9630	76.41	0.9942	0.0101	2798.74	92.06	0.006
2.94	0.0165	0.9567	76.64	0.9933	0.0205	1380.91	60.07	0.009
3.97	0.0225	0.9523	76.70	0.9912	0.0325	874.02	43.99	0.011
4.88	0.0267	0.9447	77.11	0.9892	0.0404	705.39	36.99	0.013
5.93	0.0331	0.9334	77.73	0.9869	0.0537	532.66	29.77	0.015
7.00	0.0407	0.9196	78.52	0.9824	0.0647	445.30	24.16	0.017
7.98	0.0478	0.9023	79.66	0.9755	0.0772	377.32	21.81	0.019
CO (1) + MF (2)								
p^a / MPa	$x_1{}^b$	$\rho_l{}^c$ / g·cm^{-3}	$V_{m,l}$ / cm^3·mol^{-1}	$y_1{}^b$	$\rho_g{}^c$ / g·cm^{-3}	$V_{m,g}$ / cm^3·mol^{-1}	K_1	K_2
				T/K = 293.2				
1.76	0.0184	0.9763	60.90	0.9929	0.0192	1470.19	53.88	0.009
2.50	0.0214	0.9761	60.82	0.9923	0.0215	1313.80	46.28	0.010
3.15	0.0274	0.9749	60.70	0.9915	0.0252	1121.92	34.83	0.011
4.08	0.0342	0.9713	60.70	0.9907	0.0356	794.89	26.56	0.012
5.10	0.0445	0.9647	60.77	0.9896	0.0482	587.83	20.80	0.013
6.06	0.0540	0.9547	61.09	0.9879	0.0613	463.10	17.31	0.014
7.83	0.0735	0.9325	61.87	0.9841	0.0943	302.33	13.11	0.018
8.95	0.0914	0.9112	62.69	0.9786	0.1161	247.08	11.76	0.023
				T/K = 313.2				
1.65	0.0120	0.9721	61.38	0.9899	0.0132	2145.74	82.49	0.010
2.85	0.0196	0.9715	61.17	0.9887	0.0189	1500.64	50.39	0.013
3.73	0.0259	0.9693	61.10	0.9876	0.0267	1063.57	38.09	0.014
4.81	0.0358	0.9624	61.20	0.9868	0.0391	726.93	26.05	0.016
5.95	0.0473	0.9508	61.56	0.9849	0.0548	519.78	20.79	0.017
7.10	0.0598	0.9373	62.02	0.9829	0.0742	384.74	16.40	0.020
8.06	0.0691	0.9247	62.54	0.9796	0.0941	304.50	14.15	0.024
8.96	0.0812	0.9043	63.53	0.9753	0.1112	258.92	12.44	0.028

dx.doi.org/10.1021/je3001969 | J. Chem. Eng. Data 2012, 57, 1887−1893

Table 2. continued

CO (1) + MF (2)								
p^a / MPa	$x_1{}^b$	$\rho_l{}^c$ / g·cm^{-3}	$V_{m,l}$ / cm^3·mol^{-1}	$y_1{}^b$	$\rho_g{}^c$ / g·cm^{-3}	$V_{m,g}$ / cm^3·mol^{-1}	K_1	K_2
				T/K = 333.2				
1.78	0.0101	0.9692	61.62	0.9879	0.0123	2307.95	97.81	0.012
2.63	0.0136	0.9687	61.54	0.9868	0.0140	2030.22	72.49	0.014
3.56	0.0204	0.9676	61.39	0.9849	0.0208	1369.42	48.20	0.017
4.66	0.0286	0.9607	61.55	0.9835	0.0332	859.30	34.32	0.019
5.74	0.0412	0.9478	61.96	0.9818	0.0455	628.20	23.80	0.020
6.58	0.0496	0.9375	62.36	0.9798	0.0603	475.08	19.73	0.022
7.79	0.0613	0.9230	62.93	0.9764	0.0826	348.14	15.17	0.026
8.86	0.0744	0.9013	63.98	0.9723	0.1043	276.97	13.07	0.030
				T/K = 353.2				
1.89	0.0063	0.9646	62.04	0.9851	0.0103	2764.81	156.37	0.015
2.71	0.0100	0.9642	61.95	0.9843	0.0112	2544.93	98.33	0.017
3.65	0.0159	0.9632	61.82	0.9825	0.0169	1689.99	61.64	0.020
4.43	0.0224	0.9568	62.01	0.9811	0.0259	1104.47	43.71	0.022
5.21	0.0297	0.9487	62.29	0.9792	0.0346	828.52	31.52	0.024
6.36	0.0401	0.9353	62.83	0.9769	0.0493	582.97	22.13	0.025
7.75	0.0549	0.9168	63.58	0.9733	0.0736	392.06	16.23	0.030
8.98	0.0696	0.8958	64.54	0.9688	0.0984	294.72	13.92	0.034

[a]Uncertainty of pressure: 0.01 MPa. [b]Uncertainty of mole fraction: 0.1 %. [c]Uncertainty of the density: 0.5 %.

of CO (1) + PA (2) and CO (1) + MF (2). The equilibrium ratios (K factors) as follows are also listed in Table 2.

$$K_1 = \frac{y_1}{x_1} \quad \text{and} \quad K_2 = \frac{y_2}{x_2} = \frac{1 - y_1}{1 - x_1} \tag{14}$$

Table 3 presents comparisons of the correlated results by PR EOS and PRSV EOS with van der Waals I or Panagiotopoulos–Reid mixing rules with the experimental results along with the interaction parameters. In Table 3, it is shown that the calculated

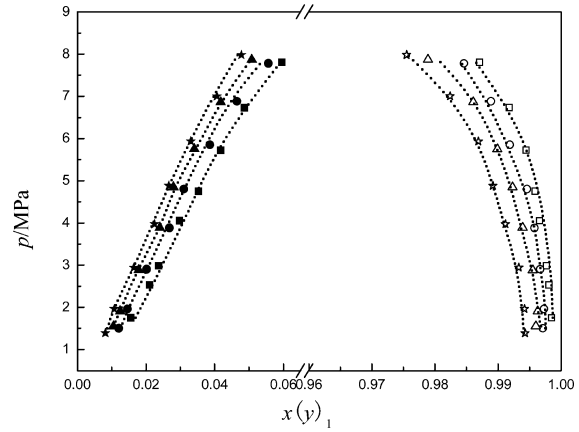

Figure 2. p–$x(y)_1$ diagrams of the CO (1) + PA (2) system. Symbols represent experimental data (solid points represent the liquid phase; unfilled points represent the vapor phase): ■, □, 293.2 K; ●, ○, 313.2 K; ▲, △, 333.2 K; ★, ☆, 353.2 K; dotted lines represent the correlation results from the PRSV equation with the Panagiotopoulos–Reid mixing rule.

results were in good agreement with the experimental data. The largest relative error of pressure (p) was 3.72 %, and that of the molar fraction of CO in the vapor phase (y) was 0.89 %. The comparisons indicated that the parameters obtained were reasonable and the correlation methods were suitable to these two binary systems. The comparisons also showed that the model

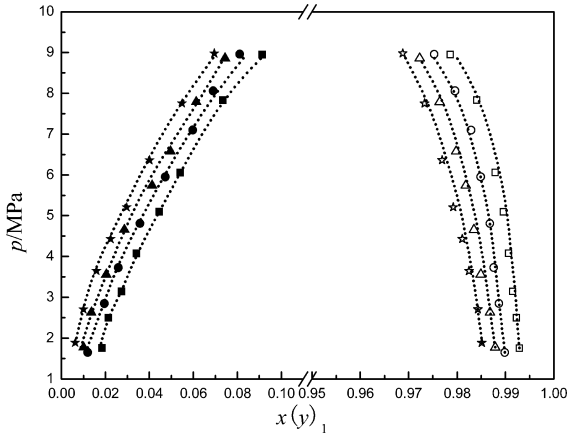

Figure 3. p–$x(y)_1$ diagrams of the CO (1) + MF (2) system. Symbols represent experimental data (solid points represent the liquid phase; unfilled points represent the vapor phase): ■, □, 293.2 K; ●, ○, 313.2 K; ▲, △, 333.2 K; ★, ☆, 353.2 K; dotted lines represent the correlation results from the PRSV equation with the Panagiotopoulos–Reid mixing rule.

of PRSV-EOS with the Panagiotopoulos–Reid mixing rule presented the best performances.

The p–x_1 (y_1), p–ρ, and V_m–x_1 (y_1) curves for CO (1) + PA (2) and CO (1) + MF (2) systems are presented in Figures 2 to 7, respectively. In the figures, the points represented the experimental data, and the dashed lines represented the correlated results by PRSV-EOS with the Panagiotopoulos–Reid mixing rule. From the figures, it can be seen that both the solubilities of CO in PA or MF and that of PA or MF in CO all rose when the pressure were increased, which resulted in the decrease of densities in the liquid phase and increase of densities in the vapor phase. The molar volume of the vapor phase decreased sharply with increasing pressure, while there were no remarkable changes for the liquid phase.

In our experiment range, the gas-phase nonideality and the nonideality due to solute–solvent interactions can be neglected, as the experimental temperatures are higher than the critical

dx.doi.org/10.1021/je3001969 | J. Chem. Eng. Data 2012, 57, 1887–1893

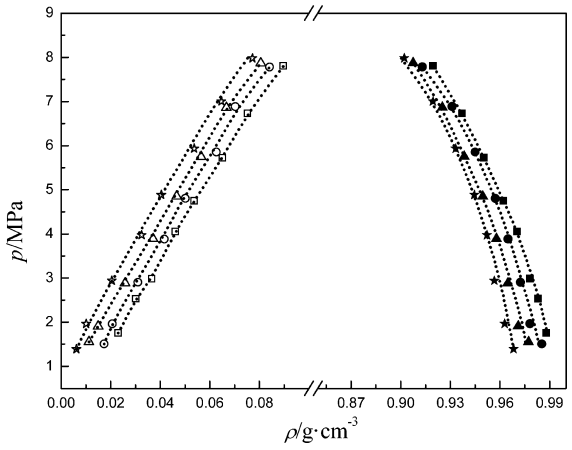

Figure 4. $p-\rho$ diagrams of the CO (1) + PA (2) system. Symbols represent experimental data (solid points represent the liquid phase; unfilled points represent the vapor phase): ■, □, 293.2 K; ●, ○, 313.2 K; ▲, △, 333.2 K; ★, ☆, 353.2 K; dotted lines represent the correlation results from the PRSV equation with the Panagiotopoulos–Reid mixing rule.

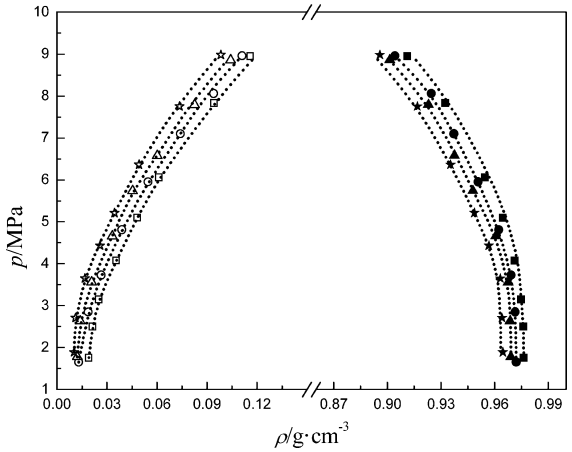

Figure 5. $p-\rho$ diagrams of the CO (1) + MF (2) system. Symbols represent experimental data (solid points represent the liquid phase; unfilled points represent the vapor phase): ■, □, 293.2 K; ●, ○, 313.2 K; ▲, △, 333.2 K; ★, ☆, 353.2 K; dotted lines represent the correlation results from the PRSV equation with the Panagiotopoulos–Reid mixing rule.

temperature of CO and the pressures are not very high. Henry's law is as follows:

$$p_i = Hx_i\gamma_i \tag{15}$$

Since the solubility of CO in PA or MF is very small ($x_1 \leq 0.0914$), we can set $\gamma_1 = 1$. Therefore,

$$H = \frac{p_1}{x_1} \tag{16}$$

The calculated Henry's coefficients at different temperatures for CO (1) + PA (2) and CO (1) + MF (2) systems are listed in Table 4. In Table 4, it is shown that Henry's coefficients of CO in both PA and MF all increased with increasing temperature in the temperature range we studied, which can be also observed in other systems.[18]

From Gibbs–Helmholtz equation, the molar solution enthalpy or molar solution entropy of the gaseous solute in the liquid phase can be calculated. If there are no specific chemical interactions and solvations between solute and solvent, they can be obtained by the equations

$$\left\{\frac{\partial \ln x_B}{\partial(1/T)}\right\}_p = -\frac{\Delta_{sol}H_B}{R} \tag{17}$$

and

$$\left\{\frac{\partial \ln x_B}{\partial \ln T}\right\}_p = \frac{\Delta_{sol}S_B}{R} \tag{18}$$

Table 3. Fitting Results for the Systems CO (1) + PA (2) and CO (1) + MF (2)

CO (1) + PA (2)					
method	T/K	k_{12}	k_{21}	$p_{ARE}{}^a$/%	$y_{ARE}{}^b$/%
PR + van der Waals I	293.2	−0.11	−0.11	3.50	0.79
	313.2	−0.28	−0.28	3.72	0.42
	333.2	0.45	0.45	3.44	0.53
	353.2	−0.41	−0.41	3.09	0.66
PRSV + van der Waals I	293.2	−0.50	−0.50	1.53	0.45
	313.2	0.50	0.50	1.25	0.31
	333.2	−0.43	−0.43	1.12	0.39
	353.2	−0.27	−0.27	1.08	0.28
PR + Panagiotopoulos–Reid	293.2	−0.14	0.36	2.58	0.55
	313.2	−0.10	0.17	2.60	0.30
	333.2	−0.05	0.11	1.99	0.37
	353.2	0.03	−0.33	2.03	0.42
PRSV + Panagiotopoulos–Reid	293.2	−0.01	0.26	1.29	0.36
	313.2	0.04	−0.20	1.20	0.27
	333.2	0.12	−0.45	1.06	0.24
	353.2	0.21	−0.47	1.06	0.25
CO (1) + MF (2)					
method	T/K	k_{12}	k_{21}	$p_{ARE}{}^a$/%	$y_{ARE}{}^b$/%
PR + van der Waals I	293.2	−0.58	−0.58	3.60	0.89
	313.2	−0.31	−0.31	3.41	0.76
	333.2	−0.22	−0.22	3.06	0.45
	353.2	−0.27	−0.27	3.85	0.63
PRSV + van der Waals I	293.2	−0.18	−0.18	1.45	0.36
	313.2	0.15	0.15	1.67	0.47
	333.2	−0.36	−0.36	1.88	0.33
	353.2	0.14	0.14	1.03	0.37
PR + Panagiotopoulos–Reid	293.2	0.03	−0.50	2.51	0.43
	313.2	−0.14	0.37	2.24	0.48
	333.2	0.15	−0.29	1.87	0.45
	353.2	−0.31	0.42	1.53	0.32
PRSV + Panagiotopoulos–Reid	293.2	0.13	0.42	1.28	0.32
	313.2	0.24	−0.23	1.39	0.33
	333.2	−0.26	0.17	1.57	0.24
	353.2	−0.41	0.28	1.04	0.29

[a]Average relative errors of p:

$$p_{ARE} = \left(\sum_{i=1}^{n}\left|\frac{p_{exp,i} - p_{cal,i}}{p_{exp,i}}\right|\right)/n$$

[b]Average relative errors of y:

$$y_{ARE} = \left(\sum_{i=1}^{n}\left|\frac{y_{exp,i} - y_{cal,i}}{y_{exp,i}}\right|\right)/n$$

dx.doi.org/10.1021/je3001969 | J. Chem. Eng. Data 2012, 57, 1887–1893

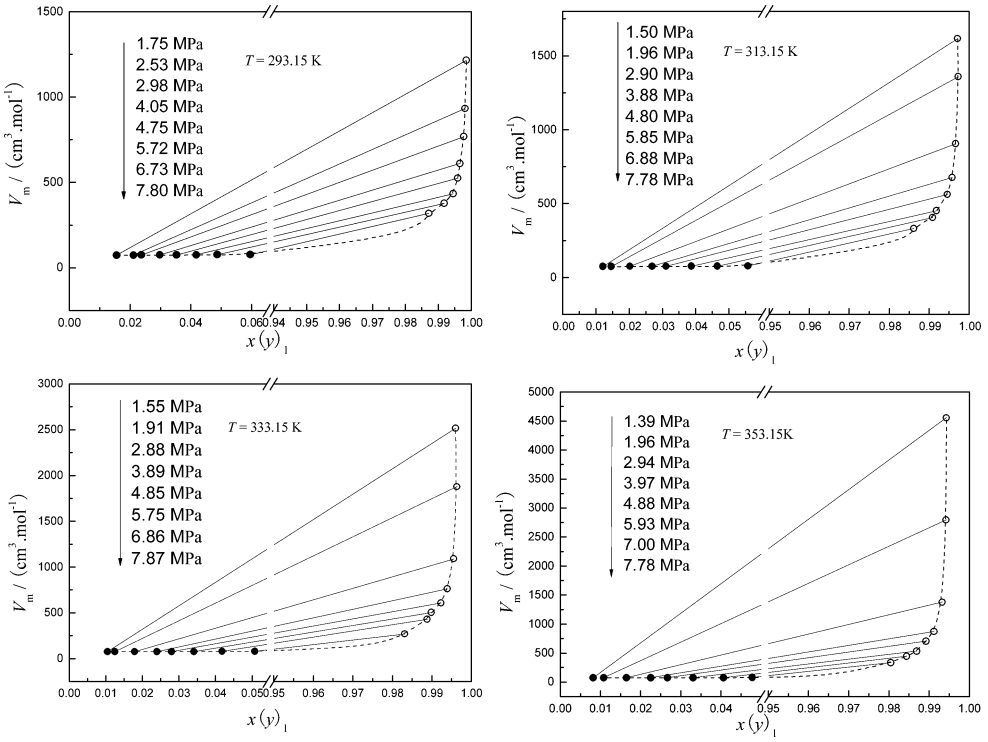

Figure 6. Isothermal V_m−$x_1(y_1)$ diagrams of the CO (1) + PA (2) system at (293.2, 313.2, 333.2, and 353.2) K. Symbols represent experimental data (solid points represent the liquid phase; hollow points represent the vapor phase); dashed lines are correlation results from the PRSV equation with the Panagiotopoulos−Reid mixing rule.

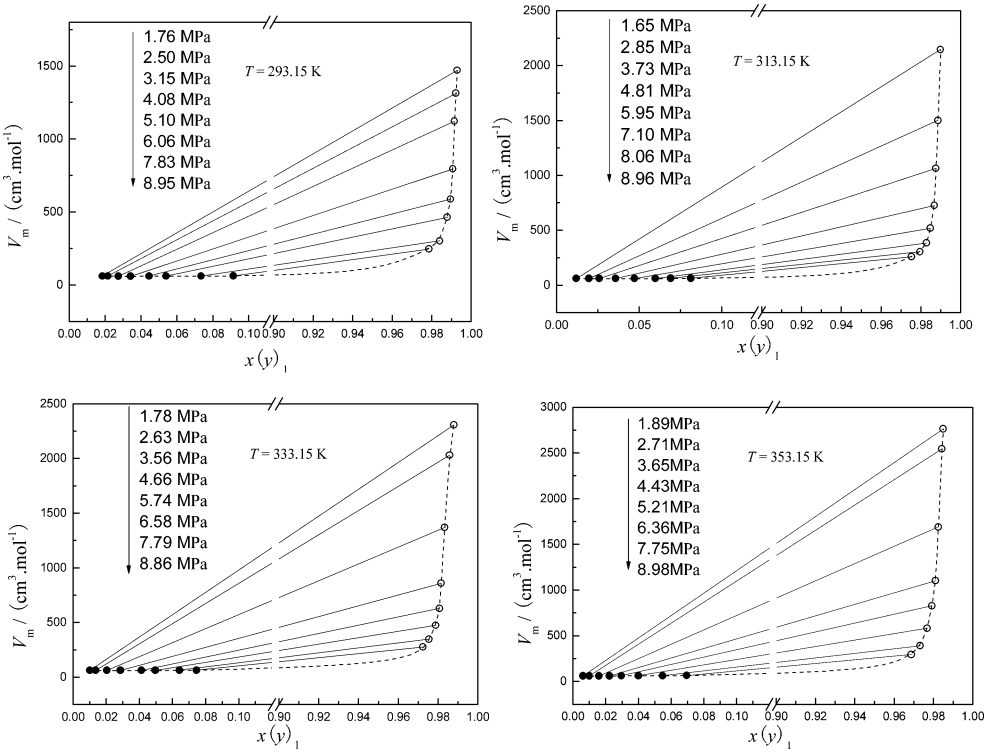

Figure 7. Isothermal V_m−$x_1(y_1)$ diagrams of the CO (1) + MF (2) system at (293.2, 313.2, 333.2, and 353.2) K. Symbols represent experimental data (solid points represent the liquid phase; hollow points represent the vapor phase); dashed lines are correlation results from the PRSV equation with the Panagiotopoulos−Reid mixing rule.

where x_B is the mole fraction of gaseous solute, $\Delta_{sol}H_B$ and $\Delta_{sol}S_B$ are the molar solution enthalpy and molar solution entropy of the gaseous solute in the liquid phase, respectively.

By fitting the relations of ln x_B with $1/T$ and ln x_B with ln T, $\Delta_{sol}H_B$, and $\Delta_{sol}S_B$ were calculated and are listed in Table 5. In Table 5, it is shown that $\Delta_{sol}H_B$ and $\Delta_{sol}H_B$ were all negative for

dx.doi.org/10.1021/je3001969 | J. Chem. Eng. Data 2012, 57, 1887−1893

Table 4. Henry's Coefficients H of CO in PA and CO in MF at Different Temperatures

		CO in PA		
T/K	293.2	313.2	333.2	353.2
H/MPa	150	160	166	177
		CO in MF		
T/K	293.2	313.2	333.2	353.2
H/MPa	93	96	100	108

Table 5. Molar Solution Enthalpy ($\Delta_{sol}H_B$) and Molar Solution Entropy ($\Delta_{sol}S_B$) of CO in PA and CO in MF at Different Pressures

p/MPa	$\Delta_{sol}H_B$/kJ·mol^{-1}	$\Delta_{sol}S_B$/J·mol^{-1}·K^{-1}
	CO in PA	
3.00	−5.04	−15.69
4.00	−4.36	−13.59
5.00	−3.95	−12.30
6.00	−3.68	−11.44
	CO in MF	
3.00	−11.92	−37.26
4.00	−7.99	−24.94
5.00	−6.17	−19.25
6.00	−5.11	−15.95

the two systems. That is to say the solubility of CO in PA or MF will decrease if the temperature is increased, which was the same as the experimental results. The difference of the cohesive energy densities is very small. The condensation of pure solute dominates the dissolution process of CO.

CONCLUSIONS

Vapor−liquid equilibrium data for the binary systems of (CO + PA) and (CO + MF) were measured. The temperature range was from (293.2 to 353.2) K, and pressure range was from (1.39 to 9.96) MPa. The results showed that, at a given temperature, both the solubilities of CO in PA or MF and that of PA or MF in CO all increased with rising pressure, which results in the decrease of densities in the liquid phase and increase of densities in the vapor phase.

The experimental data were also correlated using the PR-EOS and PRSV-EOS with the van der Waals I or Panagiotopoulos−Reid mixing rules and obtained good agreements. The compared results showed that the model of PRSV-EOS with Panagiotopoulos−Reid mixing rule presented the best performances. Furthermore, the Henry's coefficient (H), molar solution enthalpy ($\Delta_{sol}H_B$), and molar solution entropy ($\Delta_{sol}S_B$) of CO dissolving in PA or MF were calculated.

AUTHOR INFORMATION

Corresponding Author

*Tel.: +86 22 27406140; fax: +86 22 27403475; e-mail: zhurongjiao@tju.edu.cn.

Funding

The authors are grateful to the Independent Innovation Fund of Tianjin University (60302013) for supporting this research.

Notes

The authors declare no competing financial interest.

REFERENCES

(1) Zhang, A.; Yang, S. Propionic acid production from glycerol by metabolically engineered Propionibacterium acidipropionici. *Process Biochem.* **2009**, *44*, 1346−1351.

(2) Lee, J.; Kim, J.; Kim, Y. Methyl formate as a new building block in C1 chemistry. *Appl. Catal.* **1990**, *57*, 1−30.

(3) Zhang, Q.; Wang, H.; Sun, G.; Huang, K.; Fang, W.; Yang, Y. Promoting effect of CeO_2 addition to Ni/AC catalyst for vapor phase carbonylation of ethanol to propionic acid. *Catal. Commun.* **2009**, *10*, 1796−1799.

(4) Gérard, E.; Götz, H.; Pellegrini, S.; Castanet, Y.; Mortreux, A. Epoxide-tertiary amine combinations as efficient catalysts for methanol carbonylation into methyl formate in the presence of carbon dioxide. *Appl. Catal., A* **1998**, *170*, 297−306.

(5) Guzman, J.; Van, H.; Whitmire, K. Metal Cluster Catalysis: A Kinetic and Mechanistic Study of the Carbonylation of Methanol to Give Methyl Formate as Catalyzed by $[Et_4N]_2[Fe_3(CO)_9E]$ (E = S, Se, Te). *Organometallics* **2003**, *22*, 1914−1922.

(6) Choi, S.; Lee, J.; Kim, Y. An efficient ruthenium complex catalyst for the carbonylation of methanol to methyl formate. *J. Mol. Catal.* **1993**, *85*, L109−L116.

(7) Gorshkov, S.; Lin, G.; Rozovskii, A.; Serov, Y.; Uhm, S. Hydrogen diffusion through a Pd-Ru membrane in the course of methanol dehydrogenation to methyl formate on a copper-containing catalyst. *Kinet. Catal.* **1999**, *40*, 93−99.

(8) Li, W.; Liu, H.; Iglesia, E. Structures and properties of zirconia-supported ruthenium oxide catalysts for the selective oxidation of methanol to methyl formate. *J. Phys. Chem. B* **2006**, *110*, 23337−23342.

(9) He, L.; Liu, H.; Xiao, C.; Kou, Y. Liquid-phase synthesis of methyl formate via heterogeneous carbonylation of methanol over a soluble copper nanocluster catalyst. *Green Chem.* **2008**, *10*, 619−622.

(10) Prausnitz, J.; Lichtenthaler, R.; DeAzevedo, E. *Molecular Thermodynamics of Fluid Phase Equilibria*, 3rd ed.; Prentice Hall PTR: Upper Saddle River, NJ, 1999.

(11) Han, F.; Xue, Y.; Tian, Y. Vapor-liquid equilibria of carbon dioxide + acetone system at pressure from (2.36−11.77) MPa and temperature from (333.2−393.15) K. *J. Chem. Eng. Data* **2005**, *50*, 36−39.

(12) Lentz, H.; Weber, M. ρ, V, T, x values of gas−liquid phase equilibria in the binary system methane-ammonia at pressure. *Fluid Phase Equilib.* **1994**, *93*, 363−366.

(13) Zhu, R.; Zhou, J.; Liu, S.; Ji, J.; Tian, Y. Vapor-liquid equilibrium data for the binary systems in the process of synthesizing diethyl carbonate. *Fluid Phase Equilib.* **2010**, *291*, 1−7.

(14) Peng, D.; Robinson, D. A new two-constant equation of state. *Ind. Eng. Chem. Fundam.* **1976**, *15*, 59−64.

(15) Stryjek, R.; Vera, J. PRSV: An improved Peng-Robinson equation of state for pure compounds and mixtures. *Can. J. Chem. Eng.* **1982**, *64*, 323−333.

(16) Poling, B.; Prausnitz, J.; O'Connell, J. *The properties of gases and liquids*, 5th ed.; McGraw-Hill: New York, 2001.

(17) NIST Chemical Compound Data Base. http://webbook.nist.gov/chemistry.

(18) Mantor, P. D.; Abib, O.; Song, K. Y.; Kobayashi, R. Solubility of Carbon Dioxide in Propylene Carbonate at Elevated Pressures and Higher than Ambient Temperature. *J. Chem. Eng. Data* **1982**, *27*, 243−245.